Size Dependence of Chiroptical Activity in Colloidal Quantum Dots

Assaf Ben Moshe, Daniel Szwarcman, and Gil Markovich*

School of Chemistry, Raymond and Beverly Sackler Faculty of Exact Sciences, Tel-Aviv University, Tel-Aviv 69978, Israel

ABSTRACT The synthesis of chiral penicillamine-capped CdS and CdSe quantum dots (QDs) was adjusted to control the size of the nanoparticles. This, together with size separation, allowed for simultaneous tuning of absorption, circular dichroism (CD), and fluorescence on a wide wavelength range. Band edge transitions were accompanied by circular dichroism peaks which red-shifted together with the increase in particle size. The clear correlation between absorption and CD bands as well as between absorption bands and size in semiconductor QDs was used to derive an experimental scaling law for optical activity. The decrease in the intensity of circular dichroism-to-absorption ratio (dissymmetry) with the increase in particle size was stronger than linear, probably exponential. In addition, strong material type dependence was observed. The CD line shape appeared to be sensitive to the nature of the transition and may thus serve as a tool for sorting out the electronic states of the QDs. Fluorescence-detected circular dichroism (FDCD) was introduced as a new probe of optically active fluorescent nanoparticles. The analysis of the size and material dependence of the chiroptical induction effect leads to the conclusion that it is primarily an electronic interaction effect between the adsorbed chiral molecules and the electron–hole states.

KEYWORDS: quantum dots · chirality · circular dichroism · size effects · fluorescence-detected circular dichroism

Chirality is a geometric property of structures which cannot be superimposed on their mirror images. In chemistry and biology, chirality of naturally occurring and synthetic molecules is a key aspect in structure–function relationship and is involved in a vast amount of practical and fundamental research. The two mirror images of a chiral molecule, also called enantiomers, differ in their interaction with linearly or circularly polarized electromagnetic radiation, giving rise to chiroptical activity. The major measured chiroptical effect is CD, which is the differential absorption of left and right circularly polarized light. CD spectroscopy is a widely used technique for dynamic and static structure determination of biological systems and chemical compounds.[1] Another method developed by Turner and co-workers for indirect measurement of the CD is FDCD,[2] which is useful for luminescent chiral species and may offer an improved sensitivity relative to CD.[3] Chiroptical activity in inorganic nanocrystals has been first demonstrated by Schaaff and Whetten for metal-based electronic transitions of gold clusters coated with chiral glutathione molecules.[4] This study was followed by many studies on Au[5−7] and Ag[8−10] clusters coated with several types of chiral molecules in an attempt to understand the mechanism leading to the metal chiroptical properties. Three possible mechanisms for the phenomenon were suggested by Schaaff and Whetten. First, the metal core may itself be chiral. Second, an achiral metal core and adsorption of capping molecules in a chiral pattern on the surface distort the outer metal atoms. Third, both the core and the adsorption pattern of the capping molecules are achiral. The induction of chiroptical activity in this mechanism is through an electronic interaction of the metal electrons with the capping molecules' chiral centers. Further attempts to elucidate the mechanism involved were also accompanied by theoretical work. For instance, *ab initio* methodology was developed by Noguez and Garzón to calculate the electronic level structure of gold–glutathione clusters.[11,12] They have demonstrated that the optical activity of such clusters could arise from a distortion pattern forced by the incorporation of ligands, which creates a dissymmetric field. As a result, chiroptical activity is induced in metal-based electronic transitions. This is in fact a description of more than one mechanism acting concurrently. Govorov and co-workers have proposed theoretically[13,14] and also demonstrated experimentally[15] an additional mechanism for induction of chiroptical activity in metal nanoparticles. This is through a dipolar interaction between the localized surface plasmon resonance of a metal nanoparticle and the molecular dipole of a chiral chromophore attached to it. The first demonstration for induction of chiroptical activity in semiconductor nanocrystals by Gun'ko and co-workers was an exciting development.[16] The optical properties of semiconductor QDs, such as absorption and emission of radiation, are of great interest due to their strong size dependence

* Address correspondence to gilmar@post.tau.ac.il.

Received for review August 22, 2011 and accepted October 3, 2011.

Published online October 03, 2011
10.1021/nn203234b

TABLE 1. Size Estimates of the 10 Different QD Samples Used in This Study

sample number, material type	first absorption peak (nm)	diameter (nm), by absorption peak wavelength	diameter (nm) by TEM
1 CdS	324	1.6	1.9 ± 0.3
2 CdS	334	1.8	2.1 ± 0.2
3 CdS	342	1.9	2.2 ± 0.5
4 CdS	388	3.0	3.2 ± 0.6
5 CdS	409	3.7	3.8 ± 0.9
6 CdS	425	4.3	4.5 ± 1.1
7 CdS	434	4.6	4.9 ± 1.1
8 CdSe	365	1.2	
9 CdSe	423	1.7	2.2 ± 0.3
10 CdSe	440	1.9	2.5 ± 0.5

originated in quantum confinement effects.[17] This dependence allows for comfortable manipulation and control of these properties which has made these structures promising candidates for various applications, such as light-emitting devices,[18,19] bioassays,[20,21] solar energy conversion,[22,23] and so on. In Gun'ko's work, it was shown that cadmium sulfide (CdS) QDs capped with chiral penicillamine molecules exhibited chiroptical activity (CD bands) that originated in transitions associated with the QD electronic levels. On the basis of the emissive properties of these dots, it was suggested that the dots are characterized by defect-induced rather than exciton-type emission. The CD bands appeared to correspond to the band edge transitions, but other than that, a complex structure was observed throughout the spectrum (bands were observed from 200 to 350 nm and not all were assigned to exciton transitions). It was concluded that the optical activity originates in chiral distortion of surface atoms, and this argument was later strengthened by *ab initio* calculations of the structure of the surface of these dots.[24] In the work of Kotov and co-workers,[25] the same effect was demonstrated for cadmium telluride (CdTe) QDs, where it was suggested that there is a similar topological origin of chiral centers in organic molecules and inorganic nanocrystals. In the CdTe QDs, the wavelengths of the CD bands did not correlate with band edge transitions and were significantly blue-shifted. Gun'ko and co-workers have later demonstrated[26] for cadmium selenide (CdSe) QDs that the spectral location of the CD band is correlated with band edge transitions. The emission properties were still characteristic of deep trapped states. In another relevant work by Gun'ko, Kotov, and co-workers, chiroptical activity was induced in band edge transitions of chiral CdS nanotetrapods.[27] In that work, the possibility of induction of chiroptical activity in band edge transitions was strengthened. Few other groups have demonstrated related effects such as preservation of chiroptical activity in CdTe QDs, even after the chiral surfactant molecule is replaced by an achiral one,[28] and that synthesis of CdS QDs in a ferittin template gives rise to circularly polarized

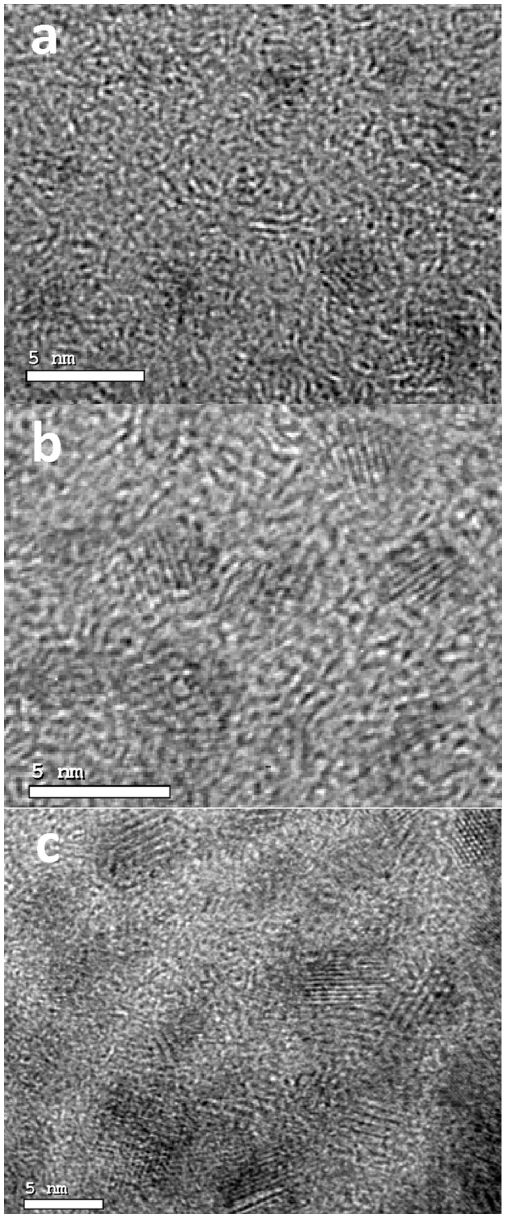

Figure 1. TEM images of (a) sample 2, (b) sample 4, and (c) sample 6 of CdS QDs. Scale bar is 5 nm for all images.

emission from these dots.[29] All previous studies relate to induction of chiroptical activity in QDs as a purely surface phenomenon and do not address the possibility of surface electronic induction on band edge transitions which originate at the core. In addition, the size and material dependence of the phenomenon were not addressed systematically since previous studies were based on a broad single size sample, without comparison of relative chiroptical intensities of the different materials.

In the present work, a size series of CdS and three sizes of CdSe QDs capped with penicillamine molecules were synthesized. It is demonstrated that after size separation and purification the CD band coincides with the band edge transitions of the dot and red shifts with size as expected of absorption and emission of

semiconductor QDs.[30] It is further demonstrated that the degree of chirotical activity (as quantified by the ratio of CD and absorption coefficients, the dissymmetry factor) strongly decreases with increase in size. An experimental evaluation of the size dependence of the dissymmetry factor is given, and it is also shown that there is a strong material dependence. The experimentally derived scaling law is discussed in light of several existing theories for the description of the phenomenon. In addition, the measurement of FDCD for QDs samples is demonstrated. This technique, which was previously used with only organic molecular systems, shows interesting results.

RESULTS AND DISCUSSION

All samples studied in this work were QDs capped with L-penicillamine molecules. The details of the samples of CdS and CdSe QDs used in this work are summarized in Table 1. The first band edge peak positions were evaluated from the second derivative of the absorption spectra. The average sizes for different samples were evaluated by transmission electron microscopy (TEM). Representative images are shown in Figure 1, showing images of samples 2 (Figure 1a), 4 (Figure 1b), and 6 (Figure 1c) of CdS QDs (examples of high-resolution images from which sizes were estimated are shown in the Supporting Information, Figure S1).

Two methods of nanocrystal size estimate were used: (1) statistics of nanoparticle diameters using high-resolution TEM; (2) using the relation between the size of the nanocrystal to the first absorption peak position which was determined experimentally by Peng and co-workers.[31] This calibration was based, for the small size regime of CdS, on results obtained by Weller and co-workers for dots synthesized in a manner similar to the present work.[32] This experimental fitting was used by many others, including the work of Kotov and co-workers on CdTe chiral QDs[25] (detailed equations appear in the Supporting Information). A rough estimation of the numbers of cadmium atoms in nanoparticles of different samples (based on bulk densities) yields ~100 atoms per nanoparticle for the smallest sample of CdS (1.6 nm) up to ~3000 atoms per nanoparticle for the largest sample of CdS (4.9 nm). The CdSe nanoparticles contained several tens of Cd atoms (sample 8) to ~200 Cd atoms (sample 10). Dynamic light scattering measurements of representative samples (Supporting Information, Figure S2) resulted in size estimates that were larger by ~0.5–1 nm from the two other methods used. This is consistent with the other sizing methods since this measurement provides the hydrodynamic radius which includes the penicillamine capping and thus less useful in discussing the core's electronic states. Nevertheless, the light scattering results verified that no significant aggregation occurred in solution.

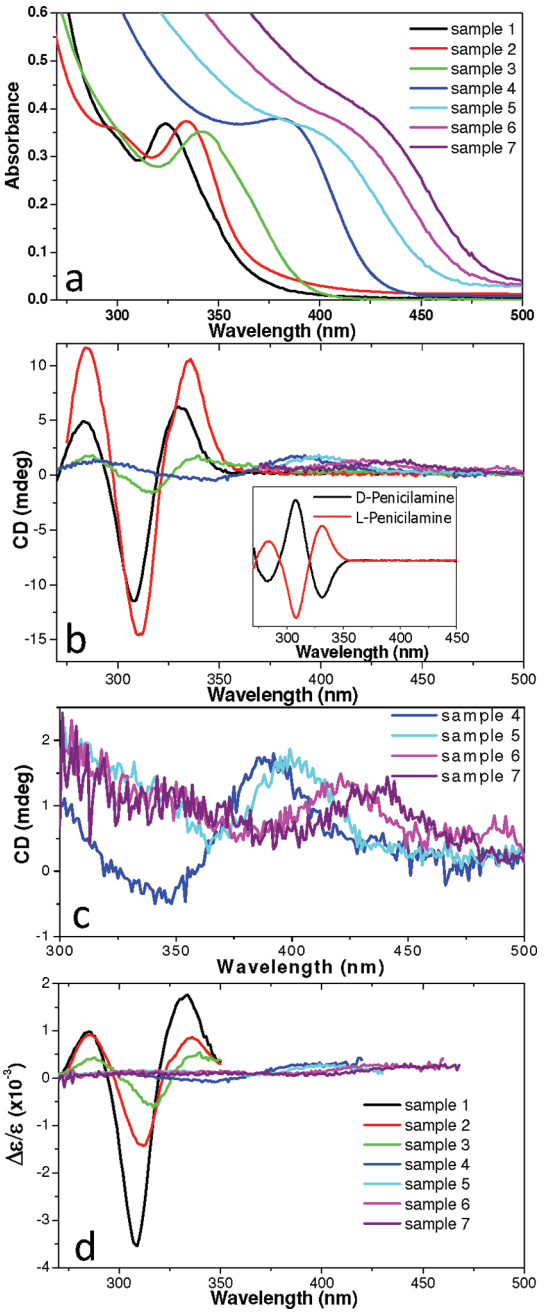

Figure 2. Absorption spectra of all CdS samples (a), CD spectra of these samples (b), magnified CD spectra of samples 4–7 (c). In the dissymmetry factor spectra plotted in (d), the spectrum of sample 5 was multiplied by 3 and the spectra of samples 6 and 7 were multiplied by 4 for clarity.

Figure 2 displays the absorption (Figure 2a) and CD (Figure 2b) spectra for CdS QDs of different sizes. Absorption spectra were scaled to the same maximum intensity for clarity (original absorption spectra appear in the Supporting Information Figure S3). The inset of Figure 2b shows that the preparation of CdS QDs with L- and D-penicillamine results in CD spectra of opposite sign, as expected. From this figure, it is evident that the first absorption peak coincides with the first positive CD peak for each size. The absorption and CD bands of

the free penicillamine molecules were monitored at different stages prior to the final addition of sulfide or selenide precursors at the exact same conditions as the actual synthesis (Supporting Information, Figure S4). The peak wavelength for absorption and CD of the free molecule was ~225 nm. No new bands at wavelengths longer than 250 nm appeared after the addition of Cd^{2+} and increase of pH. This indicates that all features observed past 300 nm were related to the electronic transitions in the quantum dots.

The dissymmetry factor spectra are plotted in Figure 2d for the various CdS sizes. The dissymmetry factor is a dimensionless measure of the strength of optical activity, which is independent of concentration and oscillator strength of the various transitions. Differential molar extinction coefficient between right and left circularly polarized light is defined by $\Delta\varepsilon = \varepsilon_L - \varepsilon_R$, where ε_R and ε_L are the absorption coefficients for right and left circularly polarized light, respectively. The dissymmetry factor is the ratio of differential to total molar absorption coefficient: $\Delta\varepsilon/\varepsilon$ (or $\Delta A/A$). The absorption and CD spectra undergo a red shift with size increase, as commonly observed for absorption and emission properties of semiconductor QDs.

Figure 3 depicts the absorption, CD, and dissymmetry of three size fractions of CdSe nanocrystals. Also, in this case, the absorption peak wavelengths match those of the CD very well. This work was limited to three samples of CdSe since, for larger size samples, the CD signal was too weak to be measured with a reasonable signal-to-noise ratio. A sample of even smaller CdSe clusters could be synthesized (see Supporting Information, Figure S5), but since the size of the core was ~1 nm, which corresponds to ~10 CdSe units, it is assumed that this sample already belongs to the molecular-like clusters regime and cannot be compared to the other quantum-dot samples.[33]

In order to better characterize the type of interaction leading to the appearance of the CD in the excitonic absorption of the QDs, the scaling of the dissymmetry factor with size was studied. The dissymmetry factor scaling was analyzed and not the CD since the concentration of particles at different samples was unknown and variations in CD intensity could result from concentration variations. Yao and co-workers studied the scaling of dissymmetry with size for chiral metal nanoparticles.[34] Such a scaling law might aid in future theoretical work to elucidate the chiroptical induction mechanism in various types of nanoparticles and, specifically, in the present work on semiconductor QDs. The benefit in deriving the scaling of dissymmetry for semiconductor nanoparticles is in the clear assignment of the first absorption and CD peak to the first allowed electron–hole pair excitation, backed by the extensive research in this field.[35,36] On the other hand, the complex CD spectrum measured for small metal clusters is difficult to directly assign to distinct absorption

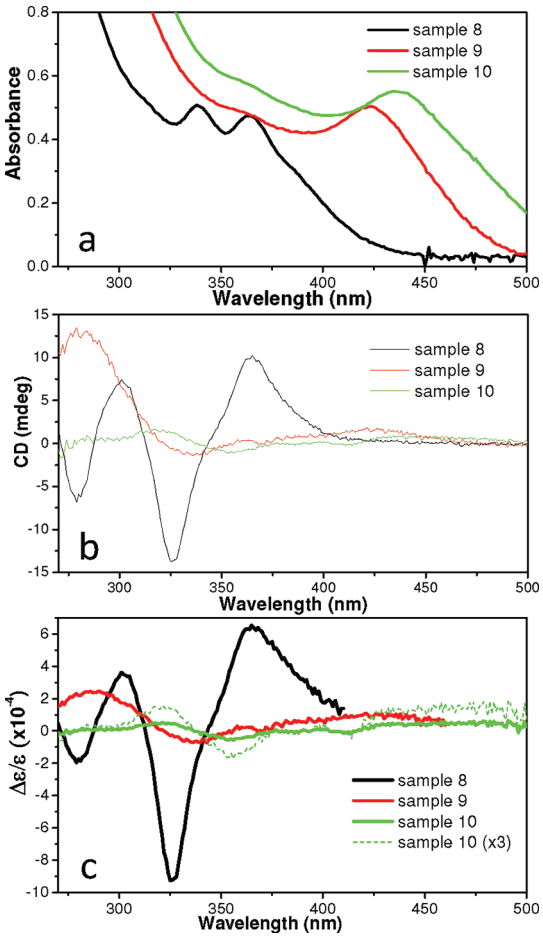

Figure 3. Absorption (a), CD (b), and dissymmetry factor (c) spectra of the three CdSe samples.

features, such as various surface plasmon resonance modes and interband transition features.

Figure 4a displays the value of the dissymmetry factor at the first absorption peak wavelength (which is roughly also the peak dissymmetry value) as a function of the inverse radius for all the CdS and CdSe samples. Two sets of CdS data are presented for both methods of size evaluation (TEM and absorption peak wavelength), which correlate well. The only difference is that TEM evaluation of size probably slightly overestimates the radii. Plotting against the inverse radius was chosen since the decrease of dissymmetry was expected to scale as the surface to volume ratio, which is proportional to the inverse radius.[16,24,25] This is under the assumption that the CD intensity is proportional to the amount of surface area (influenced by the chiral coating) and absorption is roughly proportional to nanoparticle volume. In Figure 4b, the same results for CdS (only absorption peak based size estimate) were fitted with an exponential growth as a function of $1/r$, as well as two separate linear fittings for samples 1–3 and 4–7. Interestingly, in the case of CdS, the rise of dissymmetry with the inverse radius is much stronger than a linear dependence, possibly exponential.

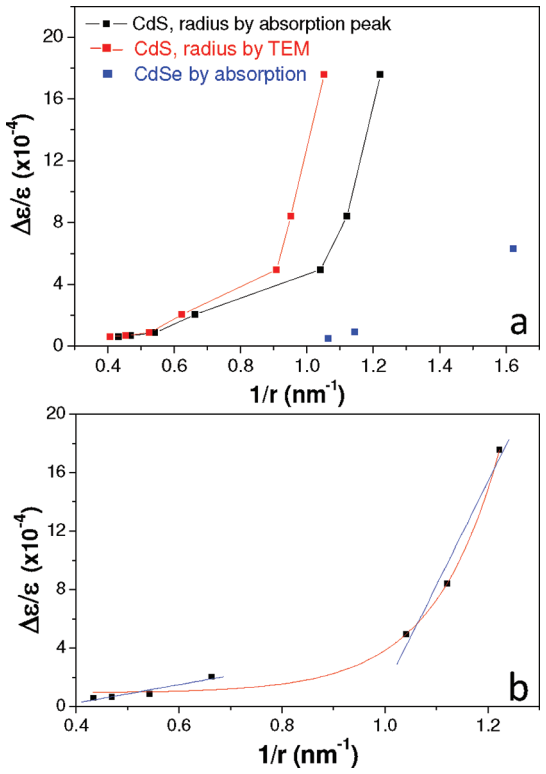

Figure 4. (a) Scaling of dissymmetry factor with inverse radius. The points corresponding to CdS represent radii derived in two ways, using TEM (red dots), and based on first absorption peak (black dots). The three CdSe samples are shown for comparison (size deduced from absorption peak). The dissymmetry factor value used here was its magnitude at the first absorption peak wavelength. (b) Dissymmetry factor as a function of inverse radius of CdS QDs (radii derived from absorption peak) with fitted exponential function, and alternatively with two separate linear fits.

Alternatively, it is also possible that the size dependence is split in two size regimes (samples 1−3 and 4−7), starting with a fast linear change at small sizes followed by a more moderate change of dissymmetry for $r > 1.5$ nm. The dissymmetry of CdSe is significantly smaller than that of CdS for comparable nanocrystal sizes, suggesting a material dependence of the phenomenon. In order to observe the sharp decrease of dissymmetry (if such exists) at very small sizes for CdSe, it appears that one will have to get to the regime of extremely small (sub-1.2 nm), molecular-like clusters, where entirely different considerations may apply.[33]

The above results can be discussed in light of previously suggested mechanisms for induction of chiroptical activity in QDs. Gun'ko and co-workers have brought experimental data and also theoretical examinations to support the induction of chiroptical activity by surface distortion in a chiral pattern,[16,24] similar to findings on gold−thiol clusters.[4−7] Kotov and co-workers have suggested a mechanism that also originates in a surface phenomenon for CdTe,[25] in which the origin of chirality is chiral centers of Cd ions with four different substituents attached, similar to the case of chiral carbon atom centers in organic molecules. This mechanism was excluded by Gun'ko and co-workers for CdS, and it was suggested that the mechanism is unique to CdTe. The present results on CdS/CdSe chiroptical effects cannot be attributed purely to surface localized states, since such states would not undergo the red shift of the CD signal with size, and due to the coincidence of the CD signal with band edge transitions. Such differences might arise from the different physical properties of CdTe. The possibility of dependence on the type of material is supported by extrapolation of the material dependence of the dissymmetry scaling. For CdTe QDs, the chiral induction on excitonic transitions might be very weak and decay very fast with size (weaker than CdSe, which is significantly weaker than CdS), leaving just the induction on surface states that behaves as described by Kotov and co-workers. This assumption is based on the CdS−CdSe−CdTe order in most physicochemical properties, such as band gap, Bohr exciton radius, and so on. Both of the previously suggested mechanisms are basically surface phenomena and a type of interaction which leads to induction on core-based excitonic transitions was not discussed so far. Both of those surface-related mechanisms are expected to result in a linear dependence of dissymmetry on inverse radius because, in these models, the CD intensity would be proportional to the number of surface chiral sites, which scales as the surface area, while the absorption scales roughly as the volume. In the current work, the results for CdS indicate that this is clearly not the case in CdS. Dissymmetry could be fitted very well with an exponential dependence of inverse radius (or a high power of this parameter). The chiroptical induction effect calculated by Noguez and Garźon for thiol−gold nanoclusters suggested that the distortion of the surface atoms and its electronic induction on the core levels cannot be separated and act concurrently.[11] A similar picture might apply in this work too, where surface atom distortion exists, but it affects the nature of the electron−hole wave functions. It is suggested in this case that the exciton wave function is strongly affected by the shell because of its delocalized nature. Additional information on such interactions can be found in previous reports on bathochromic absorption shifts in QDs. Weller and co-workers have demonstrated a reversible shift of the emission peak in CdSe nanocrystals upon ligand exchange and explained it through redistribution of electron density in the crystal following ligand exchange.[37] Weiss and co-workers have brought up the possibility for exciton−molecular orbital coupling in peptide-coated CdSe nanocrystals as an explanation for significant red shift of the absorption and emission spectra.[38] Very recently, Frederick and Weiss studied the mechanism of a similar effect in CdSe QDs.[39] Upon coordination of phenyldithiocarbamate (PTC) molecules to the surface of CdSe QDs (through cadmium−sulfur

bonds, similar to the present work's case), a significant red shift of band edge emission was observed. The mechanism proposed involves the delocalization of the hole into the organic or inorganic ligand shell. This is explained by an effective resonance between the highest occupied molecular orbital (HOMO) of the QDs and that of the PTC−Cd^{2+} molecule. In this respect, it is interesting to discuss a scenario in which the hole generated by photon absorption will partly delocalize into the chiral surface groups and hybridize with capping molecule levels. Band edge transitions to such levels are likely to be optically active. This effect should be dependent on the resonance conditions between the top of valence band of the QD and the HOMO of the surface capping molecules, which will account also for the material type dependence. A previous study by Neuhauser and co-workers on cysteine-capped CdSe clusters has indicated that such molecules induce strong electronic effects on the inorganic core-based levels.[40] It is not clear, however, without detailed calculations to what extent this report that focused on very small clusters applies to the slightly larger particles in the samples of the current work.

Induction of chiroptical activity through dipolar interactions is presumably a weak effect because of the relatively small dielectric constant of a semiconductor nanoparticle relative to that of a metallic particle.[13] However, it cannot be completely excluded without detailed calculations. In contrast to the model described in ref 13, where the separation between the centers of the chiral molecule and the nanoparticle is fairly large (of the order of nanoparticle diameter), in the present case, the small chiral molecules are attached to the nanoparticle's surface and the dipolar interaction term should have a very weak direct size dependence. The stronger dependence on size would arise from the shift in the energy levels of the QDs with size, which would change the energy separation between the molecular and QD levels and, consequently, change the magnitude of the dipolar interaction. This effect should be linearly proportional to the inverse of the energy difference between molecular transition and nanoparticle excitation.[13] In the strong confinement regime, this term would show a roughly $1/r^2$-dependent decay of CD. In addition, the dielectric constant of the nanocrystals is also size-dependent and would thus add weak size dependence to the dipolar model. Overall, the dipolar interaction is expected to have a complex polynomial dependence of dissymmetry on inverse radius but not an exponential law.

Another simple model that was previously suggested by Beratan and co-workers deals with a possibility that the surface charge creates a dissymmetric field.[41] The Coulomb interaction of the surface charges with electrons in gold clusters coated with chiral molecules was suggested to possibly induce chiroptical activity in metal-based transitions. The same possibility

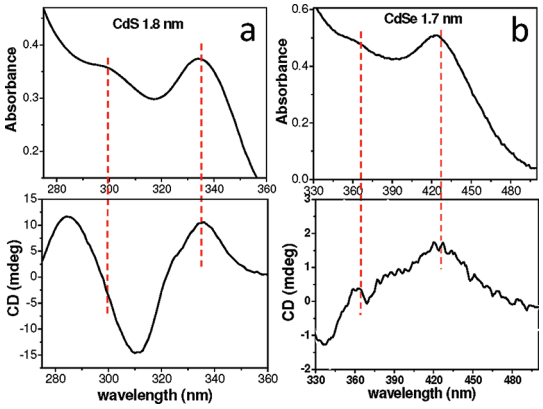

Figure 5. Absorption and CD spectra of sample 2 (CdS, 1.8 nm) (a) and sample 9 (CdSe, 1.7 nm) (b). In both samples, it is possible to observe a second excitation peak. The vertical lines highlight the correlation between the absorption peaks and CD bands.

might exist for the interaction of electrons and/or holes in semiconductor QDs with surface charges. This interaction will decay linearly with the inverse radii and induce a dissymmetry that scales with size as $1/r^4$. It was not possible to fit our data to such a power (see Supporting Information, Figure S6). The Coulomb interaction should be similar in both CdS and CdSe apart for small differences in the dielectric screening between them, which are much smaller than the observed large difference between CdS and CdSe dissymmetry factors.

It is interesting to look at the CD line shape and its relation to the different transitions observed in the absorption spectra. For that purpose, one CdS and one CdSe sample in which the CD and first absorption peak coincide and that are of narrow size distribution (according to TEM evaluations and the width of the peaks in the absorption spectrum) were chosen. The absorption and CD spectra of the two fractions are depicted in Figure 5a,b (CdS and CdSe, respectively). The positions of the first and second absorption peaks are marked by vertical lines. The first absorption peak which is associated with the first electron−hole excitation coincides with a peak in the CD spectrum. The second absorption peak exactly coincides with a zero CD value in the middle of a dissymmetric sigmoidal line shape in the case of CdS and a zero value in the middle of a weaker sigmoidal line in the case of CdSe. The different CD line shape corresponding to the second absorption peak is probably due to the different nature of this transition in the CdS and CdSe NCs (possibly different type in the two materials) relative to the first peak, such as a splitting of a multiply degenerate state due to the chiral field.

The nature of defect type emission in the current samples is verified by regular fluorescence measurements on representative CdS (Figure 6a) and CdSe (Figure 6b) samples. All samples were excited at wavelengths close to the absorption band edges. The emission undergoes a

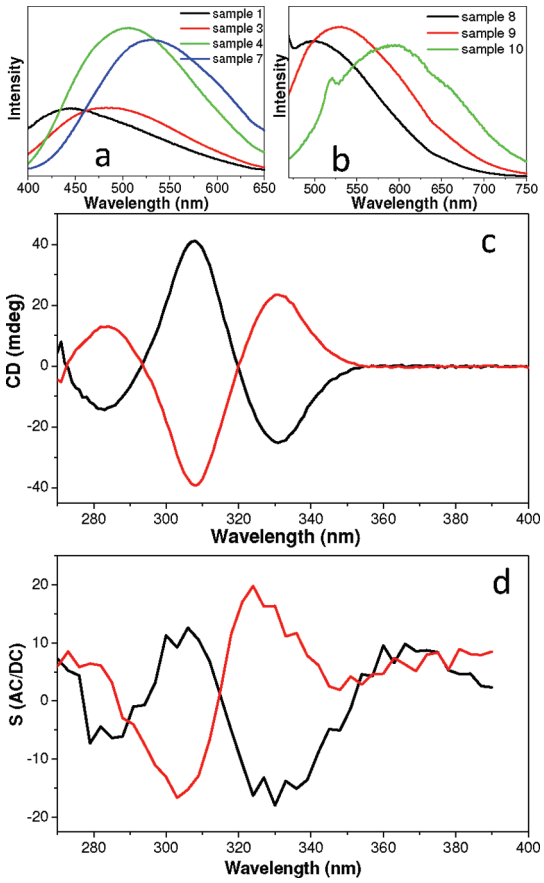

Figure 6. Emission spectra of samples 1, 3, 4, and 7 of CdS (a) and samples 8, 9, and 10 of CdSe (b) excited (correspondingly) at 340, 365, 400, 440, 380, 450, and 450 nm. CD (c) and FDCD (d) measurement results of sample 2 of CdS capped with opposite enantiomers of L/D-penicillamine. The polarities of the signals in both methods are the same.

red shift with increase in size. The large Stokes shift (on the order of ~1 eV) and broad line width of the emission suggest that the emission originates in surface trap states, as indicated by Gun'ko and co-workers.[16,24] Thus, due to the complicated nature of these emission lines, the size dependence of their properties, such as peak wavelength and width, was not studied at this point and left for future studies. FDCD measurements performed on sample 2 yielded interesting results, which could be correlated with the regular emissive properties. There is no previous information on this type of experiments for inorganic nanoparticles. The measurement was performed by placing the detector at 90° to the light source, and a 450 nm long-pass filter was used to eliminate elastically scattered excitation light. The signal in this experiment, as in the CD measurement, is the difference between the left- and right-handed polarized light reaching the detector. As a baseline, a racemic mixture of equal quantities of D- and L-penicillamine-capped CdS QDs was used because it was easily adjusted to exhibit very similar fluorescence signal as each separate enantiomer together with zero CD signal.[2]

CD (Figure 6c) spectra were of the same polarity as the FDCD spectra (Figure 6d). However, under normal circumstances, in a single luminescent transition, the polarity of the signal of the FDCD should be opposite to the normal CD signal, due to the opposite nature of absorption and emission signals, where the more absorbing enantiomer for a certain circular polarization will yield a minimum at the detector for CD measurement configuration but will also be the more emitting, leading to a maximum at the detector for FDCD measurement.[2,3] Tang and co-workers have studied the effects of different species as well as the effect of growing extinction of samples on FDCD measurements.[42] According to their findings, the same polarities of CD and FDCD signals appear at samples where a combination of fluorescent, non-optically active species and nonfluorescent, optically active species exist. The samples of chiral CdS QDs present such a complex case of multiple transitions, where the strongly absorbing core excitonic state has very poor luminescence and the surface states to which the excitation decays are luminescent but typically chiroptically inactive. Thus, the polarity of the FDCD signal leads to the important conclusion that chiroptical activity is induced on core excitonic states while, in contrast to the CdTe QDs, the surface states of the CdS are basically achiral (on average).

The surface atomic distortion influence on the chiroptical response of the inorganic core is probably different in the case of CdS in comparison to the well-studied Au–thiol system. In the R–S–Au system, the internal Au–Au bonds are very different from the covalent-like thiol–Au bond, which lead to the surface distortion.[11,12,43] In the CdS system, where the molecule–core R–S–Cd bond is basically similar to the internal ionic S–Cd bond, the distortion of the surface of the inorganic core by the penicillamine would be smaller than the Au–S case. Another consideration of the importance of the structural distortion is the QD material dependence found in this work. The Cd–Se and Cd–Te bonds are weaker than the Cd–S bond (based on bond energies in gaseous diatomic molecules),[44] and thus a surface distortion by ligand binding would probably increase on thiol binding to the surface Cd ions. These simple assumptions lead to the conclusion that the chiroptical induction should be primarily of electronic origin, and as discussed above, the strong size dependence is difficult to explain by pure electrostatic effects and would probably require a quantum description of the interaction of the extended electron–hole states with the ligand orbitals.

CONCLUSION

In this work, it was found that CD in CdS and CdSe QDs produced with chiral surfactant molecules is a size-dependent property induced on electron–hole excitations of the dots and is consequently red-shifted

with size, as expected. The possibility to tune simultaneously the absorption, emission, and CD bands of such particles might be useful for certain biosensing applications. The dissymmetry decreases with size, as expected of a surface phenomenon, but superlinearly with surface-to-volume ratio (for the case of CdS). The mechanism for induction of chiroptical activity is yet to be fully resolved, but in the future, the experimentally derived size and material dependence might be combined with *ab initio* calculations to achieve a good understanding of the mechanism. It is suggested that, other than dipolar or Coulomb interactions, quantum effects should be taken into account; namely, the delocalized nature of the electron–hole states allows for induction of chiroptical activity by the shell layer. The CD line shape of different transitions could be used for assignment of the various optical transitions and may provide a new handle for understanding the complex electronic structure of CdS QDs. This might also aid in understanding the chiroptical induction mechanism. FDCD was introduced as a new tool to probe fluorescent optically active nanoparticles. The FDCD signal's polarity was found to be useful for understanding an electronically complex system. Future research is required to better capture the origin of unexpected polarity of the FDCD signal in chiral QDs of the type presented here. Currently, the results of the FDCD support the picture of optically active, nonfluorescent exciton type transitions.

METHODS

All reagents, including L-penicillamine (99% aldrich), D-penicillamine (≥99% fluka), sodium hydroxide (ACS reagent), sodium borohydride (≥99%), cadmium perchlorate hydrate (99.999% trace metals basis), selenium (powder −100 mesh, 99.99% trace metals basis), thioacetamide (ACS reagent ≥99%), and Sephadex G-25 (coarse) were purchased from Sigma and used without any further purification. All water used was ultrapure (18 MΩ·cm), obtained from a USF ELGA UHQ system. Preparation of a size exclusion column was done by dissolving 14 g of Sephadex G-25 in 70 mL of water and stirring for one day before filling a column.

CdS QD Synthesis. Aqueous solutions of cadmium perchlorate hydrate (150 μL, 10 mM) and L-penicillamine (75 μL, 10 mM) were added to 3 mL of water under vigorous stirring. The pH of the solution was raised to ∼11.5 using aqueous sodium hydroxide solution (1 M), followed by the fast addition of aqueous thioacetamide solution (75 μL, 10 mM). The resulting sample (sample A) was left for 24 h in the dark at room temperature before loading on the size exclusion column (a C 16/40 GE Healthcare column full of Sephadex G-25). Size exclusion chromatography was mostly used to clean the samples from unreacted precursors as well as very small clusters of several atoms. For the size range of under ∼2.5 nm in diameter, it was useful for separation of sizes of QDs, as well. The column was cleaned by passing 50 mL of aqueous sodium hydroxide solution (0.32 M, pH ∼11.5) through the column at a flow rate of 30 mL/h (three repeats). Three milliliters of the sample was loaded at the same flow rate followed by loading additional 30 mL of the same sodium hydroxide solution and elution of 1 mL fractions at 30 mL/h rate. Samples 1, 2, and 3 were collected from that run. For the synthesis of samples 4–7, the as-prepared sample A was used (before size exclusion column) as seeds for further growth of the QDs. Three milliliters of sample A was vigorously stirred, and 30 portions of cadmium perchlorate and thioacetamide solutions were added at short intervals (10 μL, 10 mM of cadmium perchlorate hydrate solution and then immediately 10 μL, 10 mM of thioacetamide solution). The sample was passed through the size exclusion column under same conditions, and the final sample 4 was collected as one of the eluted fractions. Samples 5 and 6 were prepared in a similar way to sample 4 with a total of 45 (sample 5) and 60 (sample 6) and 70 (sample 7) portions of precursors added to sample A. Samples 5, 6, and 7 were centrifuged for 30 min at 15 000 rpm prior to passing them through the column. The clear yellow supernatant was collected and passed through the column, while the sediment was thrown away since it contained nanoparticle aggregates. Samples 5, 6, and 7 were collected as fractions eluted at column separations. The D-enantiomer of sample 2 was prepared by switching the L-penicillamine to D-penicillamine solution and following the same procedure described above.

CdSe QD Synthesis. Sodium hydrogen selenide was prepared by dispersing 10 mg of selenium powder in 12.6 mL of ice cold water, followed by the addition of 40 mg of sodium borohydride under vigorous stirring. The solution was used immediately after turning completely translucent. Sample 1 was prepared as follows: To 3 mL of water were added aqueous solutions of cadmium perchlorate hydrate (60 μL, 10 mM) and penicillamine (150 μL, 10 mM). The pH was raised to ∼11.5 using an aqueous solution of sodium hydroxide (1 M) and immediately followed by addition of sodium hydrogen selenide solution (60 μL, 10 mM). The sample was passed through the Sephadex column as previously described from which sample 1 was eluted as one of the fractions. The preparation of samples 2 and 3 followed exactly the same procedure, apart from a change in the quantities of the precursors: 150 μL (sample 2) and 200 μL of cadmium perchlorate hydrate and sodium hydrogen selenide solutions.

Absorption, CD, and FDCD Measurements. Absorption measurements were performed on a Varian Cary-5000 spectrophotometer. CD and FDCD measurements were performed on an Applied Photophysics Chirascan CD spectrometer. For the FDCD baseline, a racemic mixture of D- and L-penicillamine-capped QDs was used. Equal volumes of D- and L-penicillamine-capped nanoparticles of sample 2 were mixed after samples were adjusted to exhibit the same absorption intensity. The detector for the FDCD was mounted at 90° to the light source and a long-pass filter was used to cut stray excitation light at wavelengths shorter than 450 nm. The sample was diluted until the peak absorbance was ∼0.2.

Transmission Electron Microscopy (TEM). All samples for TEM were deposited on carbon-coated copper grids (SPI). Prior to deposition, the grids were placed in an ozone cleaner for 30 min, which made the carbon surface more hydrophilic. Images were recorded using a Philips FEI Tecnai F20 FEG-TEM.

Dynamic Light Scattering (DLS). DLS measurements were performed using a Malvern Instruments Nano ZS system. All samples were diluted to the same concentrations measured in the CD and absorption experiments.

Acknowledgment. This research was supported by The Israel Science Foundation Grant No. 172/10. A.B.M. and D.S. were supported by the Tel Aviv University Center for Nanoscience and Nanotechnology. The authors are grateful to Prof. A. Govorov for valuable remarks and discussion.

Supporting Information Available: Additional TEM images, DLS measurements, raw absorption and emission spectra, spectra of ultrasmall CdSe clusters, and a fit of the dissymmetry to an electrostatic model. This material is available free of charge *via* the Internet at http://pubs.acs.org.

REFERENCES AND NOTES

1. *Circular Dichroism: Principles and Applications*; Nakanishi, K., Berova, N., Woody, R. W., Eds.; Wiley-VCH: New York, 2000.
2. Turner, D. H.; Tinnoco, I., Jr.; Maestre, M. Fluorescence Detected Circular Dichroism. *J. Am. Chem. Soc.* **1974**, *96*, 4340–4343.
3. Nehira, T.; Parish, C. A.; Jockusch, S.; Turro, N. J.; Nakanishi, K.; Berova, N. Fluorescence-Detected Exciton-Coupled Circular Dichroism: Scope and Limitations in Structural Studies of Organic Molecules. *J. Am. Chem. Soc.* **1999**, *121*, 8681–8691.
4. Schaaff, T. G.; Whetten, R. L. Giant Gold−Glutathione Cluster Compounds: Intense Optical Activity in Metal-Based Transitions. *J. Phys. Chem. B* **2000**, *104*, 2630–2641.
5. Gautier, C.; Bürgi, T. Chiral *N*-Isobutyril-cysteine Protected Gold Nanoparticles: Preperation, Size Selection, and Optical Activity in the UV−Vis and Infrared. *J. Am. Chem. Soc.* **2006**, *128*, 11079–11087.
6. Yao, H.; Fukui, T.; Kimura, K. Chiroptical Responses of D-/L-Penicillamine Capped Gold Clusters under Pertubations of Temperature Change and Phase Transfer. *J. Phys. Chem. C* **2007**, *111*, 14968–14976.
7. Gautier, C.; Bürgi, T. Chiral Gold Nanoparticles. *Chem. Phys. Chem.* **2009**, *10*, 483–492.
8. Nishida, N.; Yao, H.; Kimura, K. Chiral Functionallization of Optically Inactive Monolayer-Protected Silver Nanoclusters by Chiral Ligand-Exchange Reactions. *Langmuir* **2008**, *24*, 2759–2766.
9. Yao, H.; Saeki, M.; Kimura, K. Induced Optical Activity in Boronic-Acid-Protected Silver Nanoclusters by Complexation with Chiral Fructose. *J. Phys. Chem. C* **2010**, *114*, 15909–15915.
10. Shemer, G.; Krichevski, O.; Markovich, M.; Molotsky, T.; Lubitz, I.; Kotlyar, A. B. Chirality of Silver Nanoparticles Synthesized on DNA. *J. Am. Chem. Soc.* **2006**, *128*, 11006–11007.
11. Sánchez-Castillo, A.; Noguez, C.; Garzón, I. L. On the Origin of the Optical Activity Displayed by Chiral-Ligand-Protected Metallic Nanoclusters. *J. Am. Chem. Soc.* **2010**, *132*, 1504–1505.
12. Noguez, C.; Sánchez-Castillo, A.; Hidalgo, F. Role of Morphology in the Enhanced Optical Activity of Ligand-Protected Metal Nanoparticles. *J. Phys. Chem. Lett.* **2011**, *2*, 1038–1044.
13. Govorov, A. O.; Fan, Z.; Hernandez, P.; Slocik, J. M.; Naik, R. R. Theory of Circular Dichroism of Nanomaterials Comprising Chiral Molecules and Nanocrystals: Plasmon Enhancement, Dipole Interactions, and Dielectric Effects. *Nano Lett.* **2010**, *10*, 1374–1382.
14. Govorov, A. O. Plasmon-Induced Circular Dichroism of a Chiral Molecule in the Vicinity of Metal Nanocrystals. Application to Various Geometries. *J. Phys. Chem. C* **2011**, *115*, 7914–7923.
15. Slocik, J. M.; Govorov, A. O.; Naik, R. R. Plasmonic Circualr Dichroism of Peptide-Functionalized Gold Nanoparticles. *Nano Lett.* **2011**, *11*, 701–705.
16. Moloney, M. P.; Gun'ko, Y. K.; Kelly, J. M. Chiral Highly Luminescent CdS QDs. *Chem. Commun.* **2007**, *38*, 3900–3902.
17. Alivisatos, A. P. Semiconductor Clusters, Nanocrystals, and QDs. *Science* **1996**, *271*, 933–937.
18. Kim, L.; Anikeeva, P. O.; Coe-Sullivan, S. A.; Steckel, J. S.; Bawendi, M. G.; Bulović, V. Contact Printing of QD Light-Emitting Devices. *Nano Lett.* **2008**, *8*, 4513–4517.
19. Anikeeva, P. O.; Halpert, J. E.; Bawendi, M. G.; Bulović, V. QD Light-Emitting Devices with Electroluminescence Tunable over the Entire Visible Spectrum. *Nano Lett.* **2009**, *9*, 2532–2536.
20. Fu, A. H.; Gu, W. W.; Boussert, B.; Koski, K.; Gerion, D.; Manna, L.; Le Gros, M.; Larabell, C. A.; Alivisatos, A. P. Semiconductor Quantum Rods as Single Molecule Fluorescent Biological Labels. *Nano Lett.* **2007**, *7*, 179–182.
21. Michalet, X.; Pinaud, F. F.; Bentolila, L. A.; Tsay, J. M.; Doose, S.; Li, J. J.; Sundaresan, G.; Wu, A. M.; Gambhir, S. S.; Weiss, S. QDs for Live Cells, *In Vivo* Imaging, and Diagnostics. *Science* **2005**, *307*, 538–544.
22. Yu, P.; Zhu, K.; Norman, A. G.; Ferrere, S.; Frank, A. J.; Nozik, A. J. Nanocrystalline TiO_2 Solar Cells Sensitized with InAs QDs. *J. Phys. Chem. B* **2006**, *110*, 25451–25454.
23. Raffaelle, R. P.; Castro, S. L.; Hepp, A. F.; Bailey, S. G. QD Solar Cells. *Prog. Photovoltaics: Res. Appl.* **2002**, *10*, 433–439.
24. Elliott, S. D.; Molonet, M. P.; Gun'ko, Y. K. Chiral Shells Achiral Cores in CdS QDs. *Nano Lett.* **2008**, *8*, 2452–2457.
25. Zhou, Y.; Yang, M.; Sun, K.; Tang, Z.; Kotov, N. A. Similar Topological Origin of Chiral Centers in Organic and Nanoscale Inorganic Structures: Effect of Stabilizer Chirality on Optical Isomerism and Growth of CdTe Nanocrystals. *J. Am. Chem. Soc.* **2010**, *132*, 6006–6013.
26. Gallagher, S. A.; Moloney, M. P.; Wojdyla, M.; Quinn, S. J.; Kelly, J. M.; Gun'ko, Y. K. Synthesis and Spectroscopic Studies of Chiral CdSe QDs. *J. Mater. Chem.* **2010**, *20*, 8350–8355.
27. Govan, J. E.; Jan, E.; Querejeta, A.; Kotov, N. A.; Gun'ko, Y. K. Chiral Luminescent CdS Nano-Tetrapods. *Chem. Commun.* **2010**, *46*, 6072–6074.
28. Nakashima, T.; Kobayashi, Y.; Kawai, T. Optical Activity and Chiral Memory of Thiol-Capped CdTe Nanocrystals. *J. Am. Chem. Soc.* **2009**, *131*, 10342–10343.
29. Naito, M.; Iwahori, K.; Miura, A.; Yamane, M.; Yamashita, I. Circularly Polarized Luminescent CdS QDs Prepared in a Protein Nanocage. *Angew. Chem., Int. Ed.* **2010**, *49*, 7006–7009.
30. Dabbousi, B. O.; Rodriguez-Viejo, J.; Mikulec, F. V.; Heine, J. R.; Mattoussi, H.; Ober, R.; Jensen, K. F.; Bawendi, M. G. (CdSe)ZnS Core−Shell QDs: Synthesis and Charecterization of a Size Series of Highly Luminescent Nanocrystallites. *J. Phys. Chem. B* **1997**, *101*, 9463–9475.
31. Yu, W. W.; Qu, L.; Guo, W.; Peng, X. Experimental Determination of the Extinction Coefficient of CdTe, CdSe, and CdS Nanocrystals. *Chem. Mater.* **2003**, *15*, 2854–2860.
32. Vossmeyer, T.; Katsikas, L.; Giersig, M.; Popovic, I. G.; Diesner, K.; Chemseddine, A.; Eychmüller, A.; Weller, H. CdS Nanoclusters: Synthesis, Charecterization, Size Dependent Oscillator Strength, Temperature Shift of the Excitonic Transition Energy, and Reversible Absorbance Shift. *J. Phys. Chem.* **1994**, *98*, 7665–7673.
33. Soloviev, V. N.; Eichhöffer, A.; Fenske, D.; Banin, U. Size-Dependant Optical Spectroscopy of a Homologous Series of CdSe Cluster Molecules. *J. Am. Chem. Soc.* **2001**, *123*, 2354–2364.
34. Nishida, N.; Yao, H.; Ueda, T.; Sasaki, A.; Kimura, K. Synthesis and Chiroptical Study of D/L-Penicillamine-Capped Silver Nanoclusters. *Chem. Mater.* **2007**, *19*, 2831–2841.
35. Norris, D. G.; Bawendi, M. G. Measurement and Assignment of the Size-Dependent Optical Spectrum in CdSe QDs. *Phys. Rev. B* **1996**, *53*, 16338–16346.
36. Comparelli, R.; Zezza, F.; Striccoli, M.; Curri, M. L.; Tommasi, R.; Agostiano, A. Improved Optical Properties of CdS QDs by Ligand Exchange. *Mater. Sci. Eng., C.* **2003**, *23*, 1083–1086.
37. Talapin, D. V.; Rogach, A. L.; Kornowski, A.; Hasse, M.; Weller, H. Highly Luminescent Monodisperse CdSe and CdSe/ZnS Nanocrystals Synthesized in a Hexadecylamine-Trioctylphosphine Oxide-Trioctylphosphine Mixture. *Nano Lett.* **2001**, *1*, 207–211.
38. Tsay, J. M.; Doose, S.; Pinaud, F.; Weiss, S. Enhancing the Photoluminescence of Peptide-Coated Nanocrystals with Shell Composition and UV Irradiation. *J. Phys. Chem. B* **2005**, *109*, 1669–1674.
39. Frederick, M. T.; Weiss, E. A. Relaxation of Exciton Confinement in CdSe QDs by Modification with Conjugated Dithiocarbamate Ligand. *ACS Nano* **2010**, *4*, 3195–3200.
40. Chung, S. Y.; Lee, S.; Liu, C.; Neuhauser, D. Structures and Electronic Spectra of CdSe−Cys Complexes: Density Functional Theory Study of a Simple Peptide Coated Nanocluster. *J. Phys. Chem. B* **2009**, *113*, 292–301.
41. Goldsmith, M. R.; George, C. B.; Zuber, G.; Naaman, R.; Waldeck, D. H.; Wipf, P.; Beratan, D. N. The Chiroptical Signature of Achiral Metal Clusters Induced by Dissymmetric Adsorbates. *Phys. Chem. Chem. Phys.* **2006**, *8*, 63–67.

42. White, T. G.; Pao, Y. H.; Tang, M. M. Interpretation of Fluorescence Detected Circular Dichroism Data. *J. Am. Chem. Soc.* **1975**, *97*, 4751–4753.
43. Jadzinsky, P. D.; Calero, G.; Ackerson, C. J.; Bushnell, D. A; Kornberg, R. D. Structure of a Thiol Monolayer-Protected Gold Nanoparticle at 1.1 Å Resolution. *Science* **2007**, *318*, 430–433.
44. *CRC Handbook of Chemistry and Physics*, Lide, D. R., Ed.; CRC Press Inc: Boca Raton, FL, 1995.